



Open Archive Toulouse Archive Ouverte (OATAO)

OATAO is an open access repository that collects the work of Toulouse researchers and makes it freely available over the web where possible

This is an author's version published in: <http://oatao.univ-toulouse.fr/28482>

Official URL: <https://doi.org/10.1039/d1en00455g>

To cite this version:

Liné, Clarisse^{ORCID} and Reyes-Herrera, Juan and Bakshi, Mansi^{ORCID} and Wazne, Mohammad and Costan, Valentin^{ORCID} and Roujol, David and Jamet, Elisabeth and Castillo-Michel, Hiram and Flahaut, Emmanuel^{ORCID} and Larue, Camille^{ORCID}
Fourier transform infrared spectroscopy contribution to disentangle nanomaterial (DWCNT, TiO₂) impacts on tomato plants. (2021)
Environmental Science Nano, 8 (10). 2920-2931. ISSN 2051-8153

Any correspondence concerning this service should be sent to the repository administrator: tech-oatao@listes-diff.inp-toulouse.fr

Fourier transform infrared spectroscopy contribution to disentangle nanomaterial (DWCNT, TiO₂) impacts on tomato plants†

Clarisse Liné,^{ab} Juan Reyes Herrera,^{ID}^c Mansi Bakshi,^{ad} Mohammad Wazne,^c Valentin Costa,^a David Roujol,^e Elisabeth Jamet,^e Hiram Castillo Michel,^c Emmanuel Flahaut ^{ID}^b and Camille Larue ^{ID}^{*a}

Carbon nanotubes (CNTs) and titanium dioxide nanoparticles (TiO₂-NPs) are among the most used nanomaterials (NMs). However, their impacts especially on the terrestrial ecosystems and on plants are still controversial. Apart from obvious physico-chemical differences, a possible explanation of these contrasting results could be the wide range of methods used to evaluate the toxicity at different levels of plant physiology. Fourier transformed infrared (FTIR) spectroscopy is a sensitive and widely informative technique that probes the chemical composition of plants. In this study, we investigated the impacts of CNTs and TiO₂-NPs (100 and 500 mg kg⁻¹) on tomato plants after 5, 10, 15 and 20 days of exposure in soil. Using morphological parameters, no toxicity was found except after 15 days of exposure (-57% in height and -62% in foliar area for plants exposed to 100 mg kg⁻¹ TiO₂-NPs, but no impact after CNT exposure) while FTIR revealed effects of the two NMs starting after 5 days of exposure and being maximum after 15 days. After spectral data treatment optimization, FTIR results suggested modifications in leaf cell wall components of plants subjected to both NMs. Microarray polymer profiling confirmed changes in xyloglucan and homogalacturonan levels for plants exposed to TiO₂-NPs. In summary, FTIR was an effective screening method to evaluate the impacts of NMs on tomato plants and to identify their implications on the plant cell walls.

DOI: 10.1039/d1en00455g

Environmental significance

Nanomaterial use is increasing continuously, implying their release in the environment. Today, the risk assessment of these new materials is lagging behind because of the lack of fast and reproducible techniques to assess their biological impacts. In this work, we report the use of Fourier transformed infrared (FTIR) spectroscopy as a fast, widely informative and easy to set up technique. Thanks to FTIR, early impacts of carbon nanotubes and TiO₂ nanoparticles on tomato plants exposed in soil were highlighted suggesting an alteration of plant cell walls. This information was further investigated by microarray polymer profiling confirming the relevance of FTIR data. FTIR appears thus as a very efficient technique to screen nanomaterial effects on organisms and speed up risk assessment.

^a

Laboratoire Ecologie Fonctionnelle et Environnement, CNRS, Université de Toulouse, Toulouse, France. E mail: camille.larue@ensat.fr

^b CIRIMAT, CNRS, INPT, UPS, Université de Toulouse, UMR CNRS UPS INP No.

5085, Université Toulouse 3 Paul Sabatier, Bât. CIRIMAT, 118, route de Narbonne, 31062 Toulouse cedex 9, France

^c

Beamline ID21, European Synchrotron Radiation Facility (ESRF), Grenoble, France

^d Institute of Environment and Sustainable Development, Banaras Hindu University, Varanasi, India

^e

Laboratoire de Recherche en Sciences Végétales, CNRS, UPS, Université de Toulouse, Auzeville Tolosane, France

1. Introduction

Over the last two decades, nanotechnologies have become increasingly important. Indeed, nanomaterials (NMs) present unique properties such as a large specific surface area which can be useful in many domains such as electronics, materials or food industry.¹ In 2020, the Dutch Nanodatabase revealed that a total of 5000 consumer products officially contained NMs.² Investigations about their possible use in medicine³ or in agriculture⁴ are also in progress.

Carbon nanotubes (CNTs) and titanium dioxide nanoparticles (TiO₂-NPs) are among the most widely used NMs.² CNTs are part of the carbon-based NM family. They have remarkable optical, electrical, thermal, mechanical and

chemical properties⁵ and are mainly used in batteries, plastic additives or sporting goods.⁶ TiO₂-NPs are well known for photocatalytic applications⁷ and are included for example in food additives⁸ or cosmetics.⁹ Since NM applications are steadily increasing, their release in the environment, intentionally or not, is of great concern.

Assessing NM concentrations in the environment is a major bottleneck in ecotoxicology. Modeling studies were carried out on some NMs to evaluate this information in different environmental compartments. TiO₂-NPs have been identified as one of the most concerning NMs due to the high concentrations forecast: around 61 mg kg⁻¹ in sludge treated soils against 12 µg kg⁻¹ for CNTs.¹⁰

NM impacts on terrestrial ecosystems are still controversial, in particular on plants.¹¹ Indeed, some authors reported higher germination rate and better yield after exposure to CNTs while other studies highlighted decreased root length or oxidative stress.¹¹ The same conclusions were reached for TiO₂-NP impacts on plants:¹² while some beneficial effects were reported such as a higher germination rate or increased root and shoot length,¹³⁻¹⁶ other works described decreased germination rate, plant growth or genotoxic effects.¹⁷⁻¹⁹ Until now, the specific mechanisms implied in NM uptake (active *vs.* passive, apoplast *vs.* symplast, among other questions) and impact (*e.g.* nano specific or ion related, oxidative stress mediated) are still to be identified and require further research.²⁰

Apart from obvious physico-chemical differences, a possible explanation of these contrasting phytotoxicity results may also be the method used to evaluate NM impacts on plants. Many biomarkers can be assessed from the morphological to the gene scale showing variable sensitivity. Their use to evaluate plant health is conclusive when many of them are combined. But in the literature, most of the studies use a limited number of biomarkers leading to a potentially partial image of the toxicity effects and thus a biased risk assessment. The availability of routine, standardized and widely informative analytical methods to evaluate NM toxicity is a key to fill this current gap of knowledge.²¹

Fourier transform infrared (FTIR) spectroscopy is a technique based on the vibrational state of molecules. It allows the acquisition of a spectrum combining information on a multitude of compounds, unlike chemical dosages which give access only to one compound (*e.g.* specific enzyme or secondary metabolite) after a series of reactions.²² There are two types of acquisition modes: either bulk analysis of the whole plant (few minutes per sample) or 2D-imaging mode of cross sections (few hours per map).²³ In bulk mode, sample preparation is very simple, consisting of grinding dry materials thus reducing artifacts. Therefore, FTIR is a widely informative, easy to set-up and fast technique that could be used to screen NM effects on different organisms. In plant biology, FTIR has been mainly used to characterize plant cell wall components in a highly sensitive and more time-efficient manner than traditional methods which require

isolation, extraction and fractionation of the different cell wall components.²⁴⁻²⁸ Recently, FTIR has been used in ecotoxicological studies to analyze changes occurring in biological materials after exposure to biotic or abiotic stresses.^{23,29-36} For instance, Morales *et al.*, Servin *et al.* and Zhao *et al.* highlighted changes in the chemical environment of carbohydrates of both cilantro and cucumber exposed to CeO₂, ZnO or TiO₂ NPs.^{33,35,36} Radish sprouts exposed to Ag-NPs also exhibited modifications of their IR spectral signature in the region related to lipids, proteins and particularly structural component peaks such as lignin, pectin and cellulose.³⁴ Likewise, very recently, we applied FTIR to evaluate the influence of plant species on their response to a CNT contamination highlighting the role of cell wall composition.³² Indeed, it has been demonstrated several times that cell walls play a crucial role in plant response to abiotic stresses.³⁷ Plant cell walls are composed of complex polysaccharides and a small amount of proteins and their composition can be modified in response to stress.³⁷⁻⁴⁰

However, FTIR data processing is tedious due to spectrum complexity. Indeed, it contains overlapping signals coming from many molecular bonds. A purely visual inspection of spectra is often insufficient to draw a conclusion. Several factors could weaken this analysis and its subsequent conclusions: i) sometimes, minor spectral differences not detected with the bare eye may contain critical information, ii) the baseline may vary from one sample to another, iii) instrumental noise could induce bias. For these reasons, it is important to find a way to process and analyze the data in a more systematic way using statistical approaches (*i.e.* supervised classification, clustering method) in order to obtain meaningful information.⁴¹

The main goal of this study was to develop the FTIR approach to evaluate the comparative impacts of two types of NMs (CNTs and TiO₂-NPs) taking into account: (i) different NM concentrations and (ii) different exposure durations. Seedlings of tomato (*S. lycopersicum* L.) were grown in soil contaminated with CNTs or TiO₂-NPs at two different concentrations (100 and 500 mg kg⁻¹ of soil) during different durations (5, 10, 15 and 20 days). FTIR was used as the main technique to evaluate the impact of the two NMs on tomato plants. Complementary morphological biomarkers were also assessed (height, biomass, number of leaves, leaf surface area). Finally, to better understand the FTIR data, the cell wall composition was further analyzed by microarray polymer profiling. Developing a reliable technique to assess in a screening mode the biological effects of many different types of NMs is mandatory to accelerate the risk assessment of these new materials being disseminated or intentionally introduced in our environment on a daily basis.

2. Materials and methods

2.1. Nanomaterials

TiO₂-NPs (ref 718467, Aeroxide P25, Sigma-Aldrich, Merck KGaA, Darmstadt, Germany) were characterized in a previous

experiment (same batch) and were composed of 80% anatase and 20% rutile with a nominal diameter of 25.0 ± 5.7 nm.¹⁹ They had a specific surface area of 46 ± 1 m² g⁻¹ (Fig. S1A†).¹⁹

Double walled CNTs were synthesized by catalytic chemical vapor deposition (CCVD) at 1000 °C of a mixture of CH₄ (18 mol.%) and H₂ using a Co:Mo/MgO-based catalyst (chemical composition: Mg_{0.99}Co_{0.0075}MgO_{0.0025}).⁴² The outer diameter ranged from 1 to 3 nm and the length varied from 1 to 100 microns (Fig. S1B†).⁴² The specific surface area was 980 m² g⁻¹ (Brunauer, Emmett and Teller (BET) method; Micromeritics Flow Sorb II 2300, Micromeritics, Norcross, GA, USA).

Fresh NM suspension at 1 g L⁻¹ were prepared with ultrapure water directly before use and dispersed using a sonication bath for 10 min (Elmasonic S30H, 280 W, Elma, Singen, Germany).

2.2. Soil characteristics and contamination

A silty sand soil (according to the United State Department of Agriculture⁴³) was used for this experiment (Lufa-Speyer, 2.1, Speyer, Germany) with a composition of 88.0% sand, 9.1% silt and 2.9% clay. It contained $0.71 \pm 0.08\%$ organic carbon, $0.06 \pm 0.01\%$ nitrogen, had a pH of 4.9 ± 0.3 and a cation exchange capacity of 4.3 ± 0.6 meq/100 g of soil. The soil water capacity was 60 mL/100 g of soil.

CNT or TiO₂-NP suspensions were added to the dry soil to reach a concentration of 100 or 500 mg NMs per kg dry soil (ratio liquid/soil = 1/1 in mass). After 2 h on a shaker table, the soil mixture was filtered to remove the water in excess. This soil preparation protocol ensured a soil contamination as homogeneous as possible. These concentrations were chosen to be relevant for TiO₂-NP contamination in sludge amended soils¹⁰ and comparable between NMs.

2.3. Plant material and cultivation

Organic seeds of tomato *S. lycopersicum* L. (var. Red Robin) were obtained from the French seed company Germinance (Soucelles, France) and surface-sterilized using Ca(ClO)₂ (1%). Seedlings were first grown in hydroponic conditions for 3 weeks until they reached the 5 leaf-stage. Plants were then placed into control or contaminated soil until harvest after 5, 10, 15 or 20 days of exposure. Exposure durations were chosen based on a literature study showing that more than 65% of articles studying CNT impacts on plants used exposure duration of less than 15 days.¹¹ Each exposure duration corresponded to an independent experiment. The experiments were performed in a growth chamber with controlled parameters: 10 h light/14 h dark photoperiod; 24 °C during the day and 22 °C during the night; and a hygrometry of 85%.

Five different exposure conditions were set-up: control (only soil without NM contamination), 100 mg CNTs per kg dry soil (CNT 100), 500 mg CNT per kg dry soil (CNT 500), 100 mg TiO₂-NPs per kg dry soil (TiO₂ 100) and 500 mg TiO₂-

NPs per kg dry soil (TiO₂ 500). Five biological replicates were performed in each case.

Morphological parameters were monitored every day (plant height and number of leaves). Upon harvest, other morphological parameters were measured (total fresh leaf biomass and foliar surface area using a camera and ImageJ software⁴⁴). Leaves were dried at 50 °C during 24 h prior to FTIR analysis.

2.4. FTIR analysis

About 20 mg dry leaves were ground 2×15 s at maximum speed using a FastPrep grinding machine (MP Biomedicals, Illkirch-Graffenstaden, France). Each powdered sample was analyzed in attenuated total reflectance (ATR) mode using a diamond crystal (Thermo Nicolet Nexus, Smart Orbit, Thermo Fisher Scientific, Waltham, USA). Infrared spectra were collected in the range 4000–400 cm⁻¹. All the samples (5 biological replicates) were analyzed in (technical) triplicates and each spectrum was the sum of 64 scans. OMNIC software (Thermo Fischer Scientific©) was used to export spectra.

2.5. Chemometric analysis for FTIR data

A chemometric analysis of FTIR spectra was developed using Orange software (BioLab, Ljubljana, Slovenia)⁴⁵ including the add-on Spectroscopy.⁴⁶ During the first step, data were pre-processed to eliminate possible analytical biases (such as detector noise and atmospheric background).²³ For this, a Savitzky–Golay filter was applied (point window: 21, polynomial order: 2, derivative order: 2). This filter is based on simplified least square procedures and permits removal of various instrumental and scattering effects. A vector normalization was then applied to minimize the effects of the source power fluctuations as well as to overcome variations due to the amount of leaf powder analyzed. The last step of the pre-processing was to select the region of interest in order to avoid background interferences.^{23,47} Here, we focused on two regions of the spectra: between 2900 and 2700 cm⁻¹ corresponding to the lipid region and between 1800 and 800 cm⁻¹ corresponding to the so-called fingerprint region (including proteins and polysaccharides). The region between 1800 and 2700 cm⁻¹ was removed because it mainly corresponded to background interferences. With this pre-process, the robustness and accuracy of subsequent analyses were improved and the interpretability of the data was increased by correcting issues associated with spectral data acquisition.

A multivariate analysis was then performed on the pre-processed spectra with first a principal component analysis (PCA), followed by a linear discriminant analysis (LDA) when necessary.⁴¹ PCA is an unsupervised method which searches for directions where data have the largest variance, whose results can show data structural information. While, LDA is a supervised method that looks for projections that maximize the ratio between-class to within-class. The combination of both methods is particularly useful when the number of

variables is large, especially if the number of observations (samples) is lower than the number of variables (wavenumbers) as in this work. PCA allows reducing the number of variables, in this analysis from 1246 variables to 10 components, the reduced dataset being then analyzed by LDA to enhance differences between the classes, if any.

In order to identify the wavenumbers contributing the most to differences among groups, a logistic regression was run on the pre-processed spectra. The logistic regression is a predictive model that yields the probability of occurrence of an event by fitting data to a logistic curve. The least absolute shrinkage and selection operator (LASSO) method was used to perform the regularization and feature selection. Most relevant wavenumbers were identified by obtaining logistic regression coefficients; this feature extraction method has been already used in ATR-FTIR data analysis.⁴⁸ For testing the robustness of the statistical model used, the area under a receiver operating characteristics (ROC) curve (AUC) and K-fold cross validation were used.⁴¹ Finally, to compare the different spectra among them, the area under differing absorption peaks was calculated by integrating the area starting from 0 on the pre-processed spectra.

2.6. Cell wall composition by polysaccharide microarray analysis

The cell wall composition was assessed according to Moller *et al.*⁴⁹ This technique integrates the sequential extraction of polysaccharides from cell walls, followed by generation of microarrays, which are probed with monoclonal antibodies (mAbs) with specificities for cell wall epitopes.

Cell wall polysaccharides were sequentially extracted from homogenates using three solvents: (i) 50 mM diamino-*cyclo*-hexane-tetra-acetic acid (CDTA), pH 7.5, (ii) 4 M NaOH with 1% v/v NaBH₄, and (iii) cadoxen (31% v/v 1,2-diaminoethane with 0.78 M CdO). The three extraction solvents used are known to solubilize pectins, non-cellulosic polysaccharides, and cellulose, respectively. For each extraction, a ratio of 6 μ L solvent for 1 mg fresh biomass was added to each tube before incubation with shaking for 1 h. After centrifugation at 2500g for 10 min, the supernatants were removed prior to addition of the next solvent to pellets. All the supernatants were finally stored at 4 °C. Forty μ L of diluted extracts (2/50, vol/vol) in TBS (Tris-HCl 20 mM pH 7.5, NaCl 150 mM, pH 7.0) were then loaded in each well of a Bio-Dot apparatus (BIO-RAD, Marnes-la-Coquette, France) onto nitrocellulose membranes (Sigma-Aldrich). After blocking TBS-T/BSA 0.05% (0.05% Tween), the arrays were probed overnight at 4 °C with primary mAbs directed against different cell wall epitopes (<https://plantcellwalls.leeds.ac.uk/plantprobes/>) at a 1/250 dilution (vol/vol) in TBS-T/BSA 0.05%: LM19 (for non-methylated homogalacturonans, HG), LM20 (for methylated HG, mHG), LM25 for the XLLG, XXLG and XXXG motifs of xyloglucans, XG), LM15 (for the XXXG motif of XG and to some extent single galactosyl substitution of the XXXG oligosaccharide, and LM24 (for the XLLG motif of XG). After

washing in TBS-T, the arrays were probed with anti-rat IgG secondary antibodies conjugated to alkaline phosphatase (Sigma-Aldrich) at a 1/10000 dilution (vol/vol) for 2 h before washing and developing in a BCIP/NBT (5-bromo-4-chloro-3-*g*-indolyphosphate/nitro-blue tetrazolium chloride) substrate. To check the activity of the mAbs, commercially purified polysaccharides were used as positive controls: polygalacturonic acid (HG, Sigma-Aldrich), polygalacturonic acid methyl ester (mHG, Sigma-Aldrich), and XG (Megazyme, Libios, Pontcharra-sur-Turdine, France). The arrays were scanned using an Epson Perfection V370 Photo (Nagano, Japon). Color intensity of each spot was quantified thanks to ImageJ software.

2.7. Statistical analysis

Data (morphological parameters) were checked for homoscedasticity and normality. When assumptions were met for parametric analyses, a two-way ANOVA was used. Otherwise, a Kruskal-Wallis test was applied. A PCA was also performed on the full dataset. All statistical analyses were carried out using the RStudio statistical software⁵⁰ (version 1.1.453) with multcompView,⁵¹ lsmeans,⁵² pgirmess,⁵³ ggplot2 (ref. 54) packages.

3. Results

3.1. Morphological responses

Plant height and number of leaves were recorded during the time course of the four experiments (5, 10, 15 and 20 days of exposure) as well as plant biomass and leaf area at the end of the experiments. These data are available in the ESI† (Fig. S2 and S3). No significant impact of NM exposure after 5, 10 and 20 days was evidenced for these parameters.

Differences were only detected after 15 days of exposure. Indeed, plants exposed to 100 mg kg⁻¹ TiO₂-NPs were significantly smaller than the control (57%, *p*-value < 0.05, Fig. 1A). Plants exposed to 500 mg kg⁻¹ TiO₂-NPs were 28% smaller than the control plant but this decrease was not significantly different (2.3 ± 0.3 cm for the control and 1.6 ± 0.4 cm for 500 mg kg⁻¹ TiO₂-NPs). Although plants exposed to both CNT concentrations for 15 days were not significantly different in height from the control plants, there was an increase of 26% and 28% in soils contaminated with 100 and 500 mg kg⁻¹ CNT, respectively (2.3 ± 0.3 cm for control, 2.9 ± 0.8 cm for 100 mg kg⁻¹ CNT and 2.9 ± 0.5 cm for 500 mg kg⁻¹ CNT).

The number of additional leaves at the end of the treatments was not significantly different between conditions (Fig. S2B†); plants displayed an average of 1.8 additional leaf after 15 days.

On the one hand, the total leaf area of plants exposed to the two TiO₂-NP concentrations was decreased after 15 days of exposure: 7.2 ± 2.4 cm² for 100 mg kg⁻¹ TiO₂-NPs and 8.9 ± 2.6 cm² for 500 mg kg⁻¹ TiO₂-NPs while that of the control was at 19.0 ± 2.7 cm² (*p*-value < 0.001, Fig. 1B). On the other

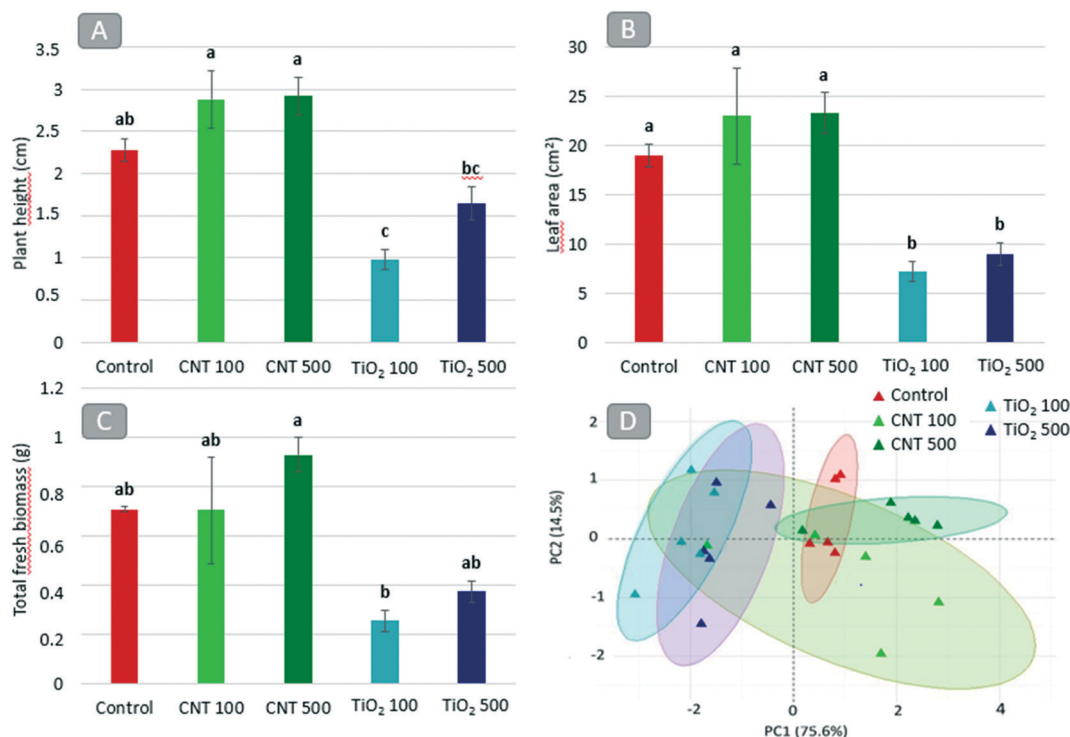


Fig. 1 Morphological responses of tomato plants: plant height (A), total leaf area (B) and total fresh biomass (C) after exposure during 15 days in soil contaminated with CNTs or TiO₂ NPs at 100 or 500 mg kg⁻¹ (CNT 100, CNT 500, TiO₂ 100, TiO₂ 500) with standard errors (*n* = 5). Different letters imply statistical differences (*p* < 0.05). D is the PCA using all the morphological parameters (leaf number, plant height, leaf area and biomass).

hand, no significant difference was found for plants exposed to CNTs.

Plant biomass was not significantly different for treated plants compared to the control after 15 days of exposure but different in between exposed plants (*p*-value < 0.001, Fig. 1C). However, plants exposed to 500 mg kg⁻¹ CNTs exhibited a trend for higher biomass compared to the control (+30%) while plants exposed to 100 mg kg⁻¹ TiO₂-NPs tended to be lighter than the control (64%).

The PCA analysis of the different morphological parameters highlighted a significant impact of TiO₂-NPs on tomato morphology after 15 days of exposure with a decrease in most of the assessed parameters while CNTs had a more mitigated impact at this developmental level (Fig. 1D).

3.2. Leaf chemical composition after FTIR analysis

Again the highest differences were visible after 15 days of treatment, even though NM impact was visible already after 5 days, opposite to what was observed from morphological parameters. PC-LDA analyses on FTIR data for 5, 10 and 20 days of NM exposure are available in ESI† (Fig. S4).

After the different contaminant exposure, the composition of leaves was significantly different between the three treatments according to the PC-LDA (Fig. 2A). Looking at the distance of the barycenter of the ellipses, the plants exposed to 500 mg kg⁻¹ CNT exhibited the highest differences in

comparison to the control while those exposed to 100 mg kg⁻¹ CNT showed the lowest differences. Both groups of the TiO₂-NP conditions were almost at the same distance from the control, but in the opposite direction to CNT groups along the component 1 axis. This result suggests that the leaf composition is different between plants exposed to CNTs and TiO₂-NPs, confirming the different impacts seen at the morphological level (decreased growth after TiO₂-NP exposure vs. trend for an increase after CNT exposure).

Once a significant cluster structure was identified for the 15 day treatment case, feature extraction was performed with a logistic regression model. This model was tested by a stratified 3-fold cross-validation method, obtaining average over classes scores of 0.932 of AUC, 0.889 of precision and a recall of 0.852, notice that a strong and robust model have scores close to one.⁴¹ A difference was highlighted in the so-called “lipid region” (Fig. 2B, peak A, Table 1) with higher relative amounts for plants exposed to the four different treatments in comparison to the control with the highest amount in leaves of plants grown on soil contaminated by CNTs at 500 mg kg⁻¹ (+ 29 ± 2.3% of the area under the peak for CNT 500 in comparison to the control). In the amide II peak,^{55,56} leaves of plants grown on contaminated soils exhibited an increase in peak area in comparison to the control except for CNT 500 (12 ± 1% increase for CNT 100, 6 ± 7% for TiO₂ 100 and 6 ± 1% TiO₂ 500) (Fig. 2B, peak B; Table 1). Polysaccharides^{38,47,56,57} also seemed to be impacted

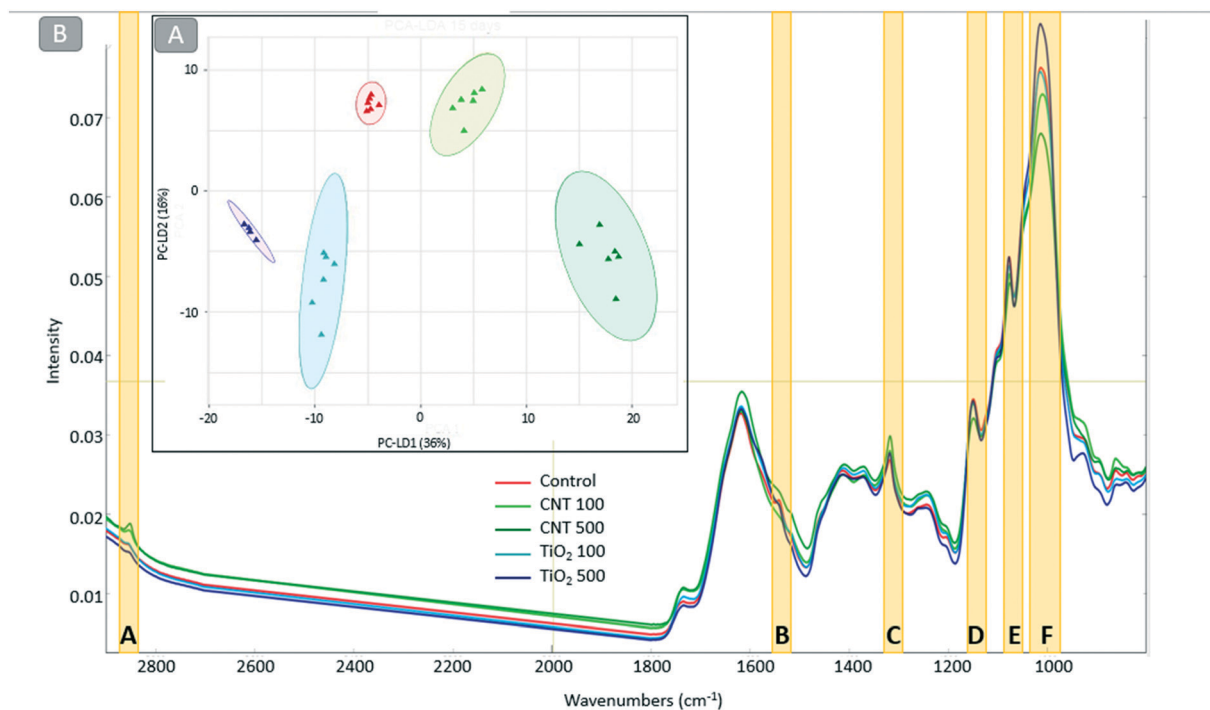


Fig. 2 (A) PC LDA analysis of the normalized FTIR spectra for tomato leaves after 15 days of exposure in soil contaminated with CNTs or TiO₂ NPs at 100 or 500 mg kg⁻¹ (CNT 100, CNT 500, TiO₂ 100, TiO₂ 500) including also the barycenter of the ellipse for each treatment. (B) Normalized FTIR spectra for tomato leaves after 15 days of exposure in soil contaminated with CNTs or TiO₂ NPs. Peaks contributing the most to differences among groups are highlighted in yellow. Peak A = 2852 2848 cm⁻¹, lipid region. Peak B = 1550 1537 cm⁻¹, amide II region. Peak C = 1320 1312 cm⁻¹, carboxyl region. Peak D = 1160 1155 cm⁻¹, polysaccharide region (cellulose). Peak E = 1082 1070 cm⁻¹, polysaccharide region (hemicelluloses). Peak F = 1052 990 cm⁻¹, pectin and various polysaccharides region.

Table 1 Peaks contributing the most to differences among treatments extracted from the logistic regression for 15 days of exposure with the band letter corresponding to the Fig. 2 together with the area under the absorption peak extracted from normalized FTIR spectra for the five different conditions (control, CNT 100, CNT 500, TiO₂ 100 and TiO₂ 500). Areas are expressed in % in comparison to the control with standard errors

Wavenumbers (cm ⁻¹)	Band	Assignment	Main compounds	Ref.	CNT 100	CNT 500	TiO ₂ 100	TiO ₂ 500	P Value
2852 2848	A	CH ₂ symmetric stretch	Lipids	47, 57	+25 ± 0%	+29 ± 2%	+12 ± 2%	+6 ± 0%	<0.001
1550 1537	B	N H and C=N	Amide II	55, 56	12 ± 1%	+1 ± 1%	-6 ± 7%	-6 ± 1%	0.041
1320 1312	C	C H bend	Carboxyl groups from ligands, proteins, various polysaccharides (cellulose)	38, 47, 56, 57	+5 ± 1%	+15 ± 3%	+3 ± 5%	+3 ± 1%	0.018
1160 1155	D	OH or C O stretch	Various polysaccharides (mainly cellulose)	38, 47, 56, 57	-1 ± 0%	-5 ± 1%	-1 ± 1%	-1 ± 1%	0.004
1082 1070	E	C O ring stretch	Various polysaccharides (hemicelluloses in particular)	38, 47, 56	-5 ± 1%	-6 ± 1%	-3 ± 1%	-1 ± 0%	0.033
1052 990	F	O H and C OH stretch	Pectin, various polysaccharides	47, 56, 57	-1 ± 2%	-6 ± 1%	+2 ± 3%	+9 ± 1%	<0.001

with differences in the areas of peaks C (1320–1312 cm⁻¹) and D (1160–1155 cm⁻¹). Exposed plants displayed an increase in peak C area while a slight decrease in the peak D area was observed. Between 1080 and 1070 cm⁻¹ corresponding to hemicellulose^{38,47,56} (Fig. 2B, peak E; Table 1), a slight decrease in the peak area was detected for the leaves of plants grown on all contaminated soils. Finally, a decrease in areas of peak F corresponding to pectin and various polysaccharides^{47,56,57} (1052–990 cm⁻¹, Fig. 2B, peak F; Table 1) was noticed for the plants grown in soil

contaminated with CNTs whereas an increase in peak F area was detected for the plants grown with TiO₂-NPs. Altogether, most of the differences observed between the FTIR spectra were related to cell wall components (pectin, cellulose or hemicellulose).

The signals obtained here were averaged on the whole leaf biomass. For further analysis, chemical composition of the leaves was observed considering their age on the two 500 mg kg⁻¹ NM treatments (Fig. 3). Overall, the oldest and the youngest (at early development stage during contaminant

exposure) leaves were the least impacted by NM contamination; leaves of plants exposed to TiO₂-NPs, in particular, had a chemical composition very similar to those of control plants (Fig. 3A and D). However, intermediate leaves (Fig. 3B and C) exposed to NM displayed different FTIR signatures than control plants, but similar in-between them according to the PC-LDA with overlapping ellipses for both CNT and TiO₂-NP treated leaves.

3.3. Cell wall composition by polysaccharide microarray analysis

As FTIR analyses suggested a strong impact of NM treatments on cell wall components, a more precise characterization was carried out on three cell wall fractions enriched in pectin, hemicellulose or cellulose. Several mAbs recognizing the main polysaccharides found in dicot cell walls were used, namely HG, mHG and different XG epitopes. No significant signal was obtained with LM20 (recognition of mHG), and LM24 (recognition of XLLG motifs of XG) mAbs (results not shown). Signals were observed with the three other mAbs: LM19 (recognition of HG), LM25 and LM15 (recognition of XLLG, XXLG and XXXG motifs and of XXXG motifs of XG, respectively) (Fig. 4).

Significant differences were found for HG (LM19) in the pectin-enriched fraction of leaves of plants exposed for 15

days to 500 mg kg⁻¹ TiO₂-NPs with a 58% increase ($p = 0.028$). The LM19 signal also increased by nearly two-fold in the hemicellulose-enriched fraction although this increase was not significant. Significant differences were also detected with LM25 for the same condition (500 mg kg⁻¹ TiO₂-NPs) in the hemicellulose-enriched fraction (+37% in comparison to the control, $p = 0.046$). However, no significant difference was found with LM15 specific for the XXXG motif of XG. It can be concluded that XXLG is the only XG motif whose amount was modified in leaves when plants were exposed to 500 mg kg⁻¹ TiO₂-NPs for 15 days. For CNT, no significant difference was found with all the mAbs tested here.

Altogether, it was not possible to detect mHG (LM19) or the XLLG motif of XG (LM24) in the tomato leaves whatever the treatment. Significant changes were only observed after the treatment with 500 mg kg⁻¹ TiO₂-NPs, corresponding to an increase in the amount of HG (LM19) and of the XXLG motif of XG (LM25, vs. LM15 and LM24).

4. Discussion

In this study, FTIR spectroscopy appeared to be a more sensitive technique to detect the impact of NM treatment on plant compared to the traditionally used morphological biomarkers. Indeed, FTIR analysis revealed a plant response to NM contamination even at the shortest time of exposure (5

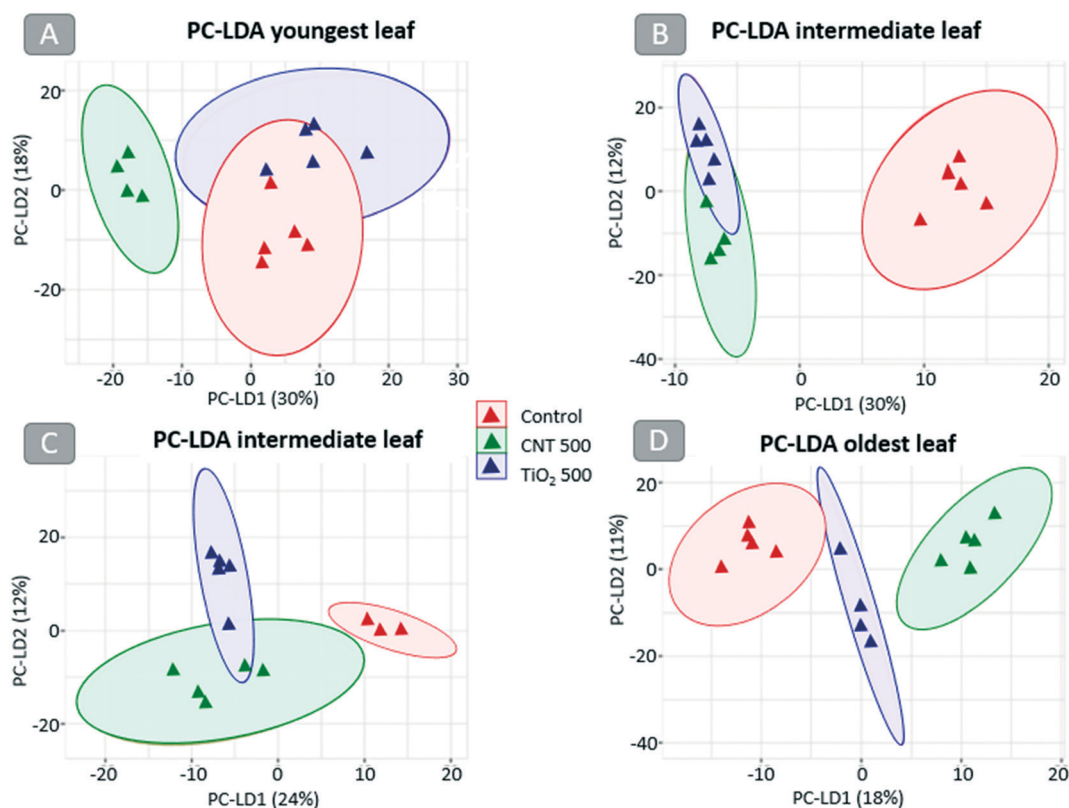


Fig. 3 PC-LDA of the FTIR spectra (between 1800 800 and 2900 2700 cm⁻¹) acquired on individual tomato leaves after 15 days of exposure in soil containing 500 mg kg⁻¹ CNTs or TiO₂ NPs (control, CNT 500 and TiO₂ 500) (A youngest leaf, B intermediate leaf, C intermediate leaf and D oldest leaf). PC-LDA were run with Orange software and drawn with RStudio (ggplot2).

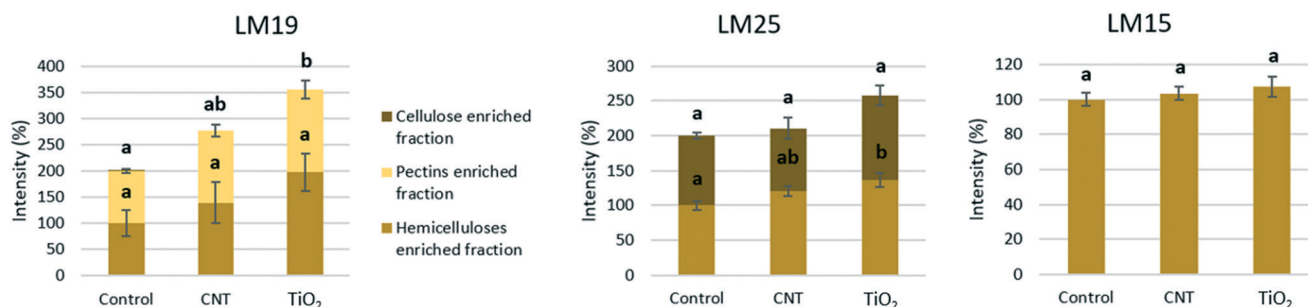


Fig. 4 Polysaccharide microarray analysis of cellulose, hemicelluloses and pectin enriched fractions of tomato cell wall leaves exposed for 15 days to 500 mg kg⁻¹ CNT or TiO₂ NPs. The detection was performed on nitrocellulose membranes which were subsequently scanned. The signals were then quantified. Results are expressed in intensity in comparison to the control and standard errors are indicated ($n = 5$). LM25 is specific for XG (motifs XLLG, XXLG and XXXG), LM15 for XG (motif XXXG) and LM19 for HG.

days). Looking at the morphological parameters, few differences were visible only after 15 days but not earlier which seemed to be compensated later. FTIR also allowed assessing NM impacts on several biomacromolecules (*i.e.* lipids, polysaccharides) in one single analysis, thus permitting to dedicate further research efforts to look at the modifications of cell wall composition under the influence of NM exposure. The developed chemometric analysis was quite powerful in highlighting differences between the experimental conditions in an automated way, which would have not been possible by visual inspection of the FTIR spectra. FTIR spectroscopy is thus a relevant method to identify early impacts of NMs on plants in a fast and reliable way, thereby permitting a screening approach.

In this soil experiment, plant response to NMs was not **dose-dependent** since most of the time, impacts were not higher at the highest concentration. One hypothesis possibly explaining this result is that NMs can have different behaviors in the environment depending on the concentration used. Indeed, when the concentration is increased, it also leads to more chances for hetero- and homo-agglomeration phenomena which would result in decreasing NM mobility and bioavailability in soils.^{58,59}

The impacts of both NMs tended to increase with **time** until 15 days of exposure, and then decreased (20 days: no detectable difference in morphological biomarkers and lower impact on biomacromolecules such as lipids, polysaccharides or proteins as demonstrated by FTIR analysis). This decrease in impacts after 15 days of exposure could suggest a plant recovery. Likewise, when studying NM impact on individual leaves of different ages, the oldest one (*i.e.* exposed for the longest period) was the least impacted in its chemical composition while clear differences were visible on other fully-expanded leaves. This could also correspond to a recovery or adaptation at the leaf level. Very little has been done so far to study plant recovery after a NM exposure. One study reported that TiO₂-NPs had no major impact on tomato plants upon harvest (after 5 months of exposure), but some markers indicated that plants might have gone through oxidative stress earlier in their life cycle.²⁹ It has also been shown after exposure to different heavy metals (Zn, Co, Cd,

Ni, Mn) that the detoxification response was triggered during the first days of exposure and then decreased back nearly to its basal level after 9 days.⁶⁰ It would thus be interesting to investigate NM impacts on biomacromolecules under chronic exposure conditions to confirm this hypothesis and further improve risk assessment strategies.

CNTs and TiO₂-NPs have been chosen here as they are two very different NMs; in particular, they vary in shape (tubular for CNTs *vs.* spherical for TiO₂-NPs), in surface chemistry (carbon *vs.* metal oxide), in diameter (1–3 nm diameter for CNTs *vs.* 25 nm for TiO₂-NPs) but they are both very insoluble. Their behavior and impacts are thus expected to be quite different. Indeed, at the morphological level, TiO₂-NPs inhibited tomato development while CNTs tended to stimulate it. These results are consistent with previously published literature.^{19,61} However, regarding biomacromolecule composition NM triggered quite similar impacts, especially on cell wall components, which might suggest a common response of plants upon exposure to CNTs or TiO₂-NPs.

FTIR spectra showed that the relative amount of lipids in leaves was increased following exposure to both NMs. This result is in agreement with studies performed on spinach, where TiO₂-NPs also increased the level of lipids after a foliar contamination.^{33,35,62} Using FTIR analysis, several studies also reported that metal-based NMs increased the relative amount of lipids in *R. sativus* (Ag-NPs)³⁴ and in *C. sativum* (CeO₂-NPs).³³ Lipid accumulation is one of the plant responses to various stresses such as high temperature, drought or heavy metals.^{63,64} Changes in the lipid composition and/or interactions between lipids and specific membrane proteins can occur in order to reinforce the phospholipid membrane to resist the stress.⁶⁵

Differences in the FTIR spectra also occurred in the protein region. Several studies reported that NMs can impact proteins (increased or decreased content; *i.e.* proteins involved in redox regulation), depending on the exposure dose and the type of plant species.⁶⁶ In particular, FTIR analysis also demonstrated a decrease in amide (both primary and secondary) in cucumber fruits and tomato leaves after exposure to TiO₂-NPs.^{29,36}

Plant cell wall components were the most impacted after exposure to both NMs. It has been reviewed several times that abiotic and biotic stresses can modify content of primary and secondary cell wall components like cellulose and hemicellulose³⁷ which can in turn influence plant growth and biomass. Indeed, it has been shown that cell wall stress feeds back to regulate microtubule organization, auxin transport, cellulose deposition, and future growth directionality.⁶⁷ For instance, in the case of drought stress, plants developed mechanisms leading to differential cell wall modifications allowing the reduction of the aerial parts while underground parts were increased to further investigate for residual water in the soil.³⁹ Here, cell walls of plants exposed to TiO₂-NPs were the most impacted and subsequently their growth was reduced up to 28% as well as their leaf area and biomass. These results are also in agreement with nanoecotoxicology studies which reported that Ag-NPs also affected cellulose and hemicellulose regions of FTIR spectra in radish sprouts (*R. sativus*).³⁴ TiO₂-NP exposure also led to an increase in the lignin band area of the FTIR spectra of cucumber fruit;³⁶ however, they decreased lignin relative content in tomato leaves but did not impact tomato fruit after exposure to TiO₂-contaminated sludge.²⁹ Cell wall components of rapeseed exposed to CNTs were also modified with a particular decrease in pectin relative amount.³² It has finally been reported that metal lignin complexes may be formed which could be responsible for changes in plant chemical environment and could lead to modifications in their nutritional properties.^{33,36}

Cellulose and hemicellulose are located inside primary cell walls and are responsible for the cell wall rigidity.³⁹ Cellulose provides mechanical strength for load-bearing due to the cross-linking by hemicelluloses.⁶⁸ Cell wall thickening represents a way for plant to resist both biotic and abiotic stress.⁴⁰ In fact, a thickening has been observed in plants as a response to mechanical intrusion of pathogens.⁶⁹ It has also been demonstrated that cellulose-deficient mutant plants are more sensitive to abiotic stress than wild type plants.³⁷ The increase in cellulose relative amount highlighted by FTIR could thus be a reaction of plant exposed to NMs to limit their entry through cell walls. This hypothesis is consistent with the result of the microarray profiling which demonstrated an increase in the LM19 labeling, *i.e.* of lowly esterified HG, also responsible for cell wall stiffening through the formation of the so-called egg boxes with calcium ions.⁷⁰

An alternative hypothesis to the increased accumulation of this cell wall component is that it represents the main negatively charged molecule of cell walls. Indeed, HG with a low degree of methylesterification contains some amount of free carboxyl groups which can bind cations. As such, it plays a crucial role as a buffer by sequestering positively charged molecules such as most heavy metals.^{40,71,72} Using quantum dots (QD, NPs with diameter <10 nm), some authors showed that NPs can directly interact with cell walls either through hydrogen bonds with cellulose -OH groups or *via* the conjugated C-C or C=C chains in lignin.^{73,74} Furthermore, a

recent study assessed the influence of NP surface charge on their fate in plants and demonstrated an accumulation of negatively charged QD in cell walls.⁷⁵ Here, both NMs bear negative charges when analyzed in suspension. However, so far, we have no data about their status in soil. Thanks to their large surface area, NMs exhibit high adsorption properties and could thus adsorb many molecules from the soil which in turn could influence their overall surface charge. In our experiment, the increase in the amount of LM19 epitopes could indicate a higher sequestration capability in response to the presence of NM in the medium.

Another phenomenon that can be responsible for cell wall modification is the oxidative stress caused by NMs. Indeed, all types of NMs (*e.g.* carbon-based and metal based) have been reported to generate an excess of reactive oxygen species (ROS).⁷⁶ For instance, CNTs increased ROS content in epidermis cells of *O. arenaria* as well as the activity of antioxidant enzymes such as peroxidases (POX) after 15 days of exposure in hydroponic conditions.⁷⁷ TiO₂-NPs also increased the level of catalase (CAT) and ascorbate peroxidase (APX) activities in leaves of cucumber exposed for 150 days in sandy loam soil.³⁶ Besides, ROS can be associated with cell wall modifications since a sudden burst of ROS can lead to catalytic oxidation of various substrates of the cell wall which results in cross-linking of cell wall components and growth arrest.⁷⁸ Class III peroxidases, also involved in the regulation of oxidative stress, can promote cell wall loosening *via* the hydroxylic cycle.⁴⁹ Indeed, this has been demonstrated in *A. thaliana* exposed to nZVI (nano zero valent iron) in agar medium.⁷⁹ The authors concluded that root elongation was related to the potential for nZVI to lead to H₂O₂ release causing OH radical-induced cell wall loosening in roots. This was confirmed by the degradation of pectin-polysaccharides and a decrease in cell wall thickness. The modification identified in the cell wall compounds in this work may thus also be explained by the oxidative stress caused by the NMs tested which could be independent of NM internalization.

5. Conclusion

The use of FTIR spectroscopy in this study has allowed to identify similar impacts of CNTs and TiO₂-NPs on tomato leaf cell walls despite their different physico-chemical properties. Microarray profiling confirmed FTIR results and demonstrated significant modification in HG and XG for plants exposed to TiO₂-NPs associated with a transiently reduced plant development (particularly visible after 15 days of exposure). The same trend in cell wall modification was noticed for plants exposed to CNTs, though not significantly, and with no impact on plant development. FTIR is a relatively easily accessible, fast and powerful technique for a first screening approach. Although data processing is not straightforward, we have proposed a strategy based on simple statistical analysis of the data which highlighted very slight modifications induced by NM exposure and permitted us to

focus the analysis further on the cell wall composition for a more precise description of the physiological response.

Conflicts of interest

Authors have no competing interests to declare.

Acknowledgements

Clarisse Liné received a grant from the Région Occitanie and the Université Fédérale de Toulouse. Mansi Bakshi was supported by Toulouse Tech InterLab funding (SPECPLANP).

Notes and references

- 1 J. Jeevanandam, A. Barhoum, Y. S. Chan, A. Dufresne and M. K. Danquah, Review on nanoparticles and nanostructured materials: history, sources, toxicity and regulations, *Beilstein J. Nanotechnol.*, 2018, **9**(1), 1050–1074, DOI: 10.3762/bjnano.9.98.
- 2 Danish Consumer Council, *The Ecological council DE, Welcome to The Nanodatabase*, <https://nanodb.dk/en/search-database/>, Published 2020, Accessed December 16, 2020.
- 3 L. García-Hevia, R. Valiente and J. L. Fernández-Luna, *et al.* Inhibition of cancer cell migration by multiwalled carbon nanotubes, *Adv. Healthcare Mater.*, 2015, **4**(11), 1640–1644, DOI: 10.1002/adhm.201500252.
- 4 J. S. Duhan, R. Kumar, N. Kumar, P. Kaur, K. Nehra and S. Duhan, Nanotechnology: The new perspective in precision agriculture, *Biotechnol. Rep.*, 2017, **15**, 11–23, DOI: 10.1016/j.btre.2017.03.002.
- 5 M. S. Dresselhaus, G. Dresselhaus and P. Avouris, *Carbon Nanotubes: Synthesis, Structure, Properties, and Applications*, Springer Science & Business Media, 2003 DOI: 10.1007/3-540-39947-X.
- 6 M. Terrones, Carbon nanotubes: synthesis and properties, electronic devices and other emerging applications, *Int. Mater. Rev.*, 2004, **49**(6), 325–377, DOI: 10.1179/174328004X5655.
- 7 S. M. Gupta and M. Tripathi, A review of TiO₂ nanoparticles, *Chin. Sci. Bull.*, 2011, **56**(16), 1639–1657, DOI: 10.1007/s11434-011-4476-1.
- 8 A. Weir, P. Westerhoff, L. Fabricius, K. Hristovski and N. von Goetz, Titanium dioxide nanoparticles in food and personal care products, *Environ. Sci. Technol.*, 2012, **46**(4), 2242–2250, DOI: 10.1021/es204168d.
- 9 P.-J. Lu, S.-C. Huang, Y.-P. Chen, L.-C. Chiueh and D. Y.-C. Shih, Analysis of titanium dioxide and zinc oxide nanoparticles in cosmetics, *J. Food Drug Anal.*, 2015, **23**(3), 587–594, DOI: 10.1016/j.jfda.2015.02.009.
- 10 T. Y. Sun, N. A. Bornhöft, K. Hungerbühler and B. Nowack, Dynamic probabilistic modeling of environmental emissions of engineered nanomaterials, *Environ. Sci. Technol.*, 2016, **50**(9), 4701–4711, DOI: 10.1021/acs.est.5b05828.
- 11 C. Liné, C. Larue and E. Flahaut, Carbon nanotubes : impacts and behaviour in the terrestrial ecosystem - A review, *Carbon*, 2017, **123**, 767–785, DOI: 10.1016/j.carbon.2017.07.089.
- 12 A. Cox, P. Venkatachalam, S. Sahi and N. Sharma, Silver and titanium dioxide nanoparticle toxicity in plants: A review of current research, *Plant Physiol. Biochem.*, 2016, **107**, 147–163, DOI: 10.1016/j.plaphy.2016.05.022.
- 13 L. Zheng, F. Hong, S. Lu and C. Liu, Effect of nano-TiO₂ on strength of naturally aged seeds and growth of spinach, *Biol. Trace Elem. Res.*, 2005, **104**(1), 083–092, DOI: 10.1385/BTER:104:1:083.
- 14 L. Clément, C. Hurel and N. Marmier, Toxicity of TiO₂ nanoparticles to cladocerans, algae, rotifers and plants - Effects of size and crystalline structure, *Chemosphere*, 2013, **90**(3), 1083–1090, DOI: 10.1016/j.chemosphere.2012.09.013.
- 15 M. Hatami and M. Ghorbanpour, Nano-anatase TiO₂ modulates the germination behavior and seedling vigority of the five commercially important medicinal and aromatic plants, *J. Biol. Environ. Sci.*, 2014, **22**(8), 53–59.
- 16 C. Larue, J. Laurette and N. Herlin-Boime, *et al.*, Accumulation, translocation and impact of TiO₂ nanoparticles in wheat (*Triticum aestivum* spp.): influence of diameter and crystal phase, *Sci. Total Environ.*, 2012, **431**, 197–208, DOI: 10.1016/j.scitotenv.2012.04.073.
- 17 M. Ghosh, M. Bandyopadhyay and A. Mukherjee, Genotoxicity of titanium dioxide (TiO₂) nanoparticles at two trophic levels: Plant and human lymphocytes, *Chemosphere*, 2010, **81**(10), 1253–1262, DOI: 10.1016/j.chemosphere.2010.09.022.
- 18 M. R. Castiglione, L. Giorgetti, C. Geri and R. Cremonini, The effects of nano-TiO₂ on seed germination, development and mitosis of root tip cells of *Vicia narbonensis* L. and *Zea mays* L., *J. Nanopart. Res.*, 2011, **13**(6), 2443–2449, DOI: 10.1007/s11051-010-0135-8.
- 19 V. Vijayaraj, C. Liné and S. Cadarsi, *et al.*, Transfer and ecotoxicity of titanium dioxide nanoparticles in the terrestrial and aquatic ecosystems: a microcosm study, *Environ. Sci. Technol.*, 2018, **52**(21), 12757–12764, DOI: 10.1021/acs.est.8b02970.
- 20 P. V. L. Reddy, J. A. Hernandez-Viezcas, J. R. Peralta-Videa and J. L. Gardea-Torresdey, Lessons learned: are engineered nanomaterials toxic to terrestrial plants?, *Sci. Total Environ.*, 2016, **568**, 470–479, DOI: 10.1016/j.scitotenv.2016.06.042.
- 21 P. C. Ray, H. Yu and P. P. Fu, Toxicity and environmental risks of nanomaterials: challenges and future needs, *J. Environ. Sci. Health, Part C: Environ. Carcinog. Ecotoxicol. Rev.*, 2009, **27**(1), 1–35, DOI: 10.1080/10590500802708267.
- 22 S. Sravan Kumar, P. Manoj and P. Giridhar, Fourier transform infrared spectroscopy (FTIR) analysis, chlorophyll content and antioxidant properties of native and defatted foliage of green leafy vegetables, *J. Food Sci. Technol.*, 2015, **52**(12), 8131–8139, DOI: 10.1007/s13197-015-1959-0.
- 23 M. J. Baker, J. Trevisan and P. Bassan, *et al.*, Using Fourier transform IR spectroscopy to analyze biological materials, *Nat. Protoc.*, 2014, **9**(8), 1771–1791, DOI: 10.1038/nprot.2014.110.
- 24 M. Szymanska-Chargot and A. Zdunek, Use of FT-IR spectra and PCA to the bulk characterization of cell wall residues of fruits and vegetables along a Fraction Process, *Food Biophys.*, 2013, **8**(1), 29–42, DOI: 10.1007/s11483-012-9279-7.

- 25 A. Largo-Gosens, M. Hernandez-Altamirano, L. Garcaa-Calvo, A. Alonso-Siman, J. Alvarez and J. L. Acebes, Fourier transform mid infrared spectroscopy applications for monitoring the structural plasticity of plant cell walls, *Front. Plant Sci.*, 2014, 5, 303, DOI: 10.3389/fpls.2014.00303.
- 26 M. Chylińska, M. Szymańska-Chargot and A. Zdunek, FT-IR and FT-Raman characterization of non-cellulosic polysaccharides fractions isolated from plant cell wall, *Carbohydr. Polym.*, 2016, 154, 48–54, DOI: 10.1016/j.CARBPOL.2016.07.121.
- 27 N. Gierlinger, New insights into plant cell walls by vibrational microspectroscopy, *Appl. Spectrosc. Rev.*, 2018, 53(7), 517–551, DOI: 10.1080/05704928.2017.1363052.
- 28 M. McCann, M. Hammouri, R. Wilson, P. Belton and K. Roberts, Fourier transform infrared microspectroscopy is a new way to look at plant cell walls, *Plant Physiol.*, 1992, 100(4), 1940–1947, DOI: 10.1104/pp.100.4.1940.
- 29 M. Bakshi, C. Liné and D. E. Bedolla, *et al.* Assessing the impacts of sewage sludge amendment containing nano-TiO₂ on tomato plants: A life cycle study, *J. Hazard. Mater.*, 2019, 369, 191–198, DOI: 10.1016/j.JHAZMAT.2019.02.036.
- 30 L. Dao, J. Beardall and P. Heraud, Characterisation of Pb-induced changes and prediction of Pb exposure in microalgae using infrared spectroscopy, *Aquat. Toxicol.*, 2017, 188, 33–42, DOI: 10.1016/j.aquatox.2017.04.006.
- 31 K. Thumanu, M. Sompong, P. Phansak, K. Nontapot and N. Buensanteai, Use of infrared microspectroscopy to determine leaf biochemical composition of cassava in response to *Bacillus subtilis* CaSUT007, *J. Plant Interact.*, 2015, 10(1), 270–279, DOI: 10.1080/17429145.2015.1059957.
- 32 C. Liné, F. Manent, A. Wolinski, E. Flahaut and C. Larue, Comparative study of response of four crop species exposed to carbon nanotube contamination in soil, *Chemosphere*, 2021, 274, 129854, DOI: 10.1016/j.chemosphere.2021.129854 0045-6535.
- 33 M. I. Morales, C. M. Rico and J. Angel Hernandez-Viezas, *et al.* Toxicity assessment of cerium oxide nanoparticles in cilantro (*Coriandrum sativum* L.) plants grown in organic soil, *J. Agric. Food Chem.*, 2013, 61, 6224–6230, DOI: 10.1021/jf401628v.
- 34 N. Zuverza-Mena, R. Armendariz, J. R. Peralta-Videa and J. L. Gardea-Torresdey, Effects of silver nanoparticles on radish sprouts: root growth reduction and modifications in the nutritional value, *Front. Plant Sci.*, 2016, 7, 1–11, DOI: 10.3389/fpls.2016.00090.
- 35 L. Zhao, J. R. Peralta-Videa and C. M. Rico, *et al.* CeO₂ and ZnO nanoparticles change the nutritional qualities of cucumber (*Cucumis sativus*), *J. Agric. Food Chem.*, 2014, 62(13), 2752–2759, DOI: 10.1021/jf405476u.
- 36 A. D. Servin, M. I. Morales and H. Castillo-Michel, *et al.* Synchrotron verification of TiO₂ accumulation in cucumber fruit: a possible pathway of TiO₂ nanoparticle transfer from soil into the food chain, *Environ. Sci. Technol.*, 2013, 47(20), 11592–11598, DOI: 10.1021/es403368j.
- 37 H. Le Gall, F. Philippe, J.-M. Domon, F. Gillet, J. Pelloux and C. Rayon, Cell wall metabolism in response to abiotic stress, *Plants*, 2015, 4(1), 112–166, DOI: 10.3390/plants4010112.
- 38 A. Alonso-Simón, P. García-Angulo, H. Mélida, A. Encina, J. M. Álvarez and J. L. Acebes, The use of FTIR spectroscopy to monitor modifications in plant cell wall architecture caused by cellulose biosynthesis inhibitors, *Plant Signaling Behav.*, 2011, 6(8), 1–7, DOI: 10.4161/psb.6.8.15793.
- 39 R. Tenhaken, Cell wall remodeling under abiotic stress, *Front. Plant Sci.*, 2014, 5, 771, DOI: 10.3389/fpls.2014.00771.
- 40 M. Krzesłowska, The cell wall in plant cell response to trace metals: polysaccharide remodeling and its role in defense strategy, *Acta Physiol. Plant.*, 2011, 33, 35–51, DOI: 10.1007/s11738-010-0581-z.
- 41 R. Gautam, S. Vanga, F. Ariese and S. Umapathy, Review of multidimensional data processing approaches for Raman and infrared spectroscopy, *EPJ Tech. Instrum.*, 2015, 2(1), 8, DOI: 10.1140/epjti/s40485-015-0018-6.
- 42 E. Flahaut, R. Bacsá, A. Peigney and C. Laurent, Gram-scale CCVD synthesis of double-walled carbon nanotubes, *Chem. Commun.*, 2003(12), 1442–1443, DOI: 10.1039/B301514A.
- 43 Soil Survey Staff, *Soil taxonomy: A basic system of soil classification for making and interpreting soil surveys*, Natural Resources Conservation Service, U.S. Department of Agriculture Handbook 436, 2nd edn, 1999.
- 44 C. A. Schneider, W. S. Rasband and K. W. Eliceiri, NIH image to ImageJ: 25 years of image analysis, *Nat. Methods*, 2012, 9(7), 671–675.
- 45 J. Demšar, A. Erjavec and T. Hočevár, *et al.* *Orange: Data Mining Toolbox in Python* Tomaž Curk Matija Polajnar Laň Zagor, 2013, vol. 14.
- 46 M. Toplak, G. Birarda and S. Read, *et al.* Infrared Orange: connecting hyperspectral data with machine learning, *Synchrotron Radiat. News*, 2017, 30, 40–45.
- 47 S. Türker-Kaya and C. W. Huck, A review of mid-infrared and near-infrared imaging: principles, concepts and applications in plant tissue analysis, *Molecules*, 2017, 22, 168, DOI: 10.3390/molecules22010168.
- 48 S. M. Savassa, H. Castillo-Michel, A. E. Pradas del Real, J. Reyes-Herrera, J. P. Rodrigues Marquesa and H. W. P. de Carvalho, Ag nanoparticles enhancing *Phaseolus vulgaris* seedling development: understanding nanoparticle migration and chemical transformation across the seed coat, *Environ. Sci.: Nano*, 2021, 8, 493–501, DOI: 10.1039/d0en00959h.
- 49 I. Moller, I. Sørensen and A. J. Bernal, *et al.* High-throughput mapping of cell-wall polymers within and between plants using novel microarrays, *Plant J.*, 2007, 50, 1118–1128, DOI: 10.1111/j.1365-313X.2007.03114.x.
- 50 J. Fox, *An R and S-Plus Companion to Applied Regression*, Sage Publications, 2002.
- 51 R. V. Lenth, Least-Squares Means: The R Package lsmeans, *J. Stat. Softw.*, 2016, 69(1), 1–33, DOI: 10.18637/jss.v069.i01.
- 52 P. Giraudoux, J.-P. Antonietti, C. Beale, D. Pleydell and M. Treglia, Spatial Analysis and Data Mining for Field Ecologists [R package pgirmess version 1.6.9], *J. Stat. Softw.*, 2018, 63.
- 53 H. Wickham, *Ggplot2: Elegant Graphics for Data Analysis*, Springer, 2009.
- 54 S. Lê, J. Josse, A. Rennes and F. Husson, *FactoMineR: An R Package for Multivariate Analysis*, 2008, vol. 25.

- 55 C. Sene, M. McCann, R. Wilson and R. Grinter, Fourier-Transform Raman and Fourier-Transform Infrared Spectroscopy (An Investigation of Five Higher Plant Cell Walls and Their Components), *Plant Physiol.*, 1994, **106**(4), 1623–1631, DOI: 10.1104/pp.106.4.1623.
- 56 M. Regvar, D. Eichert, B. Kaulich, A. Gianoncelli, P. Pongrac and K. Vogel-Mikuš, Biochemical characterization of cell types within leaves of metal-hyperaccumulating *Nocca praecox* (Brassicaceae), *Plant Soil*, 2013, **373**(1–2), 157–171, DOI: 10.1007/s11104-013-1768-z.
- 57 H. Schulz and M. Baranska, Identification and quantification of valuable plant substances by IR and Raman spectroscopy, *Vib. Spectrosc.*, 2007, **43**(1), 13–25, DOI: 10.1016/j.vibspec.2006.06.001.
- 58 P. S. Tourinho, C. A. M. van Gestel, S. Lofts, C. Svendsen, A. M. V. M. Soares and S. Loureiro, Metal-based nanoparticles in soil: fate, behavior, and effects on soil invertebrates, *Environ. Toxicol. Chem.*, 2012, **31**(8), 1679–1692, DOI: 10.1002/etc.1880.
- 59 M. Baalousha, M. Sikder, A. Prasad, J. Lead, R. Merrifield and G. T. Chandler, The concentration-dependent behaviour of nanoparticles, *Environ. Chem.*, 2015, 1–4, DOI: 10.1071/EN15142.
- 60 A. Lešková, R. F. H. Giehl, A. Hartmann, A. Fargašová and N. von Wirén, Heavy metals induce iron deficiency responses at different hierarchic and regulatory levels, *Plant Physiol.*, 2017, **174**, 1648–1668, DOI: 10.1104/pp.16.01916.
- 61 M. V. Khodakovskaya, B.-S. Kim and J. N. Kim, *et al.* Carbon nanotubes as plant growth regulators: effects on tomato growth, reproductive system, and soil microbial community, *Small*, 2013, **9**(1), 115–123, DOI: 10.1002/sml.201201225.
- 62 C. M. Rico, M. I. Morales and A. C. Barrios, *et al.* Effect of cerium oxide nanoparticles on the quality of rice (*Oryza sativa* L.) grains, *Environ. Sci. Technol.*, 2013, **47**, 5635–5642, DOI: 10.1021/jf404046v.
- 63 A. Kuczyńska, V. Cardenia, P. Ogrodowicz, M. Kempa, M. T. Rodriguez-Estrada and K. Mikołajczak, Effects of multiple abiotic stresses on lipids and sterols profile in barley leaves (*Hordeum vulgare* L.), *Plant Physiol. Biochem.*, 2019, **141**, 215–224, DOI: 10.1016/j.plaphy.2019.05.033.
- 64 V. N. Nesterov, O. A. Rozentsvet and S. V. Murzaeva, Changes in lipid composition in the tissues of fresh-water plant *Hydrilla verticillata* induced by accumulation and elimination of heavy metals, *Russ. J. Plant Physiol.*, 2009, **56**, 85–93, DOI: 10.1134/S1021443709010130.
- 65 Q. Guo, L. Liu and B. Barkla, Membrane lipid remodeling in response to salinity, *Int. J. Mol. Sci.*, 2019, **20**(17), 4264, DOI: 10.3390/ijms20174264.
- 66 M. Hatami, K. Kariman and M. Ghorbanpour, Engineered nanomaterial-mediated changes in the metabolism of terrestrial plants, *Sci. Total Environ.*, 2016, **571**, 275–291, DOI: 10.1016/j.scitotenv.2016.07.184.
- 67 D. J. Cosgrove, Plant cell wall extensibility: connecting plant cell growth with cell wall structure, mechanics, and the action of wall-modifying enzymes, *J. Exp. Bot.*, 2016, **67**(2), 463–476, DOI: 10.1093/jxb/erv511.
- 68 *The Apoplast of Higher Plants: Compartment of Storage, Transport and Reactions*, ed. Sattelmacher B. and Horst W. J., Springer Netherlands, Dordrecht, 2007 DOI: 10.1007/978-1-4020-5843-1.
- 69 C. A. Voigt, Callose-mediated resistance to pathogenic intruders in plant defense-related papillae, *Front. Plant Sci.*, 2014, **5**, 168, DOI: 10.3389/fpls.2014.00168.
- 70 S. Wolf, G. Mouille and J. Pelloux, Homogalacturonan methyl-esterification and plant development, *Mol. Plant*, 2009, **2**(5), 851–860, DOI: 10.1093/mp/ssp066.
- 71 F. Schwab, G. Zhai, M. Kern, A. Turner, J. L. Schnoor and M. R. Wiesner, Barriers, pathways and processes for uptake, translocation and accumulation of nanomaterials in plants - Critical review, *Nanotoxicology*, 2016, **10**(3), 257–278, DOI: 10.3109/17435390.2015.1048326.
- 72 M. Kartel, L. Kupchik and B. Veisov, Evaluation of pectin binding of heavy metal ions in aqueous solutions, *Chemosphere*, 1999, **38**, 2591–2596.
- 73 D. Djikanović, A. Kalauzi and M. Jeremić, *et al.* Interaction of the CdSe quantum dots with plant cell walls, *Colloids Surf., B*, 2012, **91**(1), 41–47, DOI: 10.1016/j.colsurfb.2011.10.032.
- 74 H. Sun, M. Wang, C. Lei and R. Li, Cell wall: An important medium regulating the aggregation of quantum dots in maize (*Zea mays* L.) seedlings, *J. Hazard. Mater.*, 2021, **403**, 123960, DOI: 10.1016/j.jhazmat.2020.123960.
- 75 S. Majumdar, C. Ma and M. Villani, *et al.* Surface coating determines the response of soybean plants to cadmium sulfide quantum dots, *NanoImpact*, 2019, **14**, 100151, DOI: 10.1016/j.impact.2019.100151.
- 76 P. Begum and B. Fugetsu, Phytotoxicity of multi-walled carbon nanotubes on red spinach (*Amaranthus tricolor* L) and the role of ascorbic acid as an antioxidant, *J. Hazard. Mater.*, 2012, **243**, 212–222, DOI: 10.1016/j.jhazmat.2012.10.025.
- 77 E. Smirnova, A. Gusev and O. Zaytseva, *et al.* Uptake and accumulation of multiwalled carbon nanotubes change the morphometric and biochemical characteristics of *Onobrychis arenaria* seedlings, *Front. Chem. Sci. Eng.*, 2012, **6**(2), 132–138, DOI: 10.1007/s11705-012-1290-5.
- 78 F. Passardi, C. Penel and C. Dunand, Performing the paradoxical: how plant peroxidases modify the cell wall, *Trends Plant Sci.*, 2004, **9**(11), 534–540, DOI: 10.1016/J.TPLANTS.2004.09.002.
- 79 J. H. Kim, Y. Lee and E. J. Kim, *et al.* Exposure of iron nanoparticles to *Arabidopsis thaliana* enhances root elongation by triggering cell wall loosening, *Environ. Sci. Technol.*, 2014, **48**(6), 3477–3485, DOI: 10.1021/es4043462.